Chemosphere 161 (2016) 151–156

Contents lists available at ScienceDirect

Chemosphere

journal homepage: www.elsevier.com/locate/chemosphere

Submerged bed versus unsaturated flow reactor: A pressurized hydrogenotrophic denitrification reactor as a case study

Razi Epsztein*, Michael Beliavski, Sheldon Tarre, Michal Green

Faculty of Civil and Environmental Engineering, Technion – Israel Institute of Technology, Haifa 32000, Israel

HIGHLIGHTS

- Two modes of pressurized hydrogenotrophic denitrification reactor were compared.
- The unsaturated-flow mode with liquid recirculation presented higher rates and $k_L\alpha$.
- The unsaturated-flow mode with liquid recirculation presented lower effluent TSS.
- The operation under saturated-flow mode with gas recirculation was more stable.
- Energy consumption of gas recirculation is expected to be significantly lower.

ARTICLE INFO

Article history:
Received 9 May 2016
Received in revised form
29 June 2016
Accepted 2 July 2016
Available online 15 July 2016

Handling Editor: Y Liu

Keywords:
Closed-headspace reactor
Gas recirculation
Hydrogenotrophic denitrification
Liquid recirculation
Submerged bed
Unsaturated flow

ABSTRACT

The paper compares the main features of a submerged bed reactor (SuBR) with bubbling and recirculation of gas to those of an unsaturated flow reactor (uSFR) with liquid recirculation. A novel pressurized closed-headspace hydrogenotrophic denitrification system characterized by safe and economic utilization of H_2 gas was used for the comparison.

Under similar conditions, denitrification rates were lower in the SuBR as a result of a lower effective biofilm surface area and overall gas-liquid mass transfer coefficient k_La. Similar values of effluent DOC were achieved for both reactors, although effluent suspended solids concentration of the SuBR were substantially higher. On the other hand, the required cleaning frequency in the SuBR was 2.5 times lower. Moreover, the SuBR is expected to reduce the recirculation energy consumption by 0.35 kWh/m^3 treated.

1. Introduction

Treatment processes of diverse water contaminants include submerged bed reactors and unsaturated flow biofilm reactors (similar to trickling filters). Trickling filters are characterized by simplicity, high degradation efficiency, low operation costs and small footprints. One of the main disadvantage of trickling filters is the risk of clogging with the accompanying need for frequent reactor cleaning (Daigger and Boltz, 2011; Eding et al., 2006; Epsztein et al., in press; Lekang and Kleppe, 2000). In submerged systems, the bubbles scour excess sludge from the carriers by the shear forces of the turbulent gas and, therefore, submerged systems are considered less susceptible to clogging than trickling filters (Schlegel and Koeser, 2007). Another drawback of trickling filters is the high hydraulic and energy-demanding recirculation commonly applied in order to achieve full media wetting (Eding et al., 2006; Epsztein et al., in press).

A novel pressurized reactor for hydrogenotrophic denitrification of groundwater operating at high denitrification rates together with minimal hydrogen loss and low risk was recently presented (Epsztein et al., 2016). The main novelty of the reactor is the operation under a pressurized closed headspace without any gas discharge. The common concern of N_2 gas build-up in a pressurized denitrifying system is addressed by the idea that in continuous operation a gas-liquid equilibrium is achieved according to Henry's law and the effluent water carries excess N_2 gas out of the reactor.

* Corresponding author.
E-mail address: epsztein@tx.technion.ac.il (R. Epsztein).

http://dx.doi.org/10.1016/j.chemosphere.2016.07.005
0045-6535/

Nomenclature

A	effective biofilm surface area [m^2/m^3]
a	specific interfacial area [m^2/m^3]
δ	length of gas-liquid boundary layer [m]
$D_{f,H}$	diffusion coefficient of H_2 in the biofilm [m^2/d]
$D_{f,N}$	diffusion coefficient of NO_3^- in the biofilm [m^2/d]
H^*	equilibrium concentration of dissolved H_2 [mg/L]
H_e	effluent concentration of dissolved H_2 [mg/L]
$k_{0f,H}$	degradation rate of H_2 in the biofilm [g/($L_{biofilm}$·d)]
$k_{0f,N}$	degradation rate of NO_3^--N in the biofilm [g/($L_{biofilm}$·d)]
k_La	overall volumetric gas-liquid mass transfer coefficient of H_2 [1/d]
N_e	effluent NO_3^--N concentration [mg/L]
N_i	inlet NO_3^--N concentration [mg/L]
$q_{max,N}$	maximal specific degradation rate of NO_3^--N [g/(gVSS·d)]
$q_{max,H}$	maximal specific degradation rate of H_2 [g/(gVSS·d)]
Q	volumetric flow rate [mL/min]
Q_R	liquid recirculation flow rate [mL/min]
r_H	overall H_2 degradation rate [g/(L·d)]
r_N	overall NO_3^-—N degradation rate [g/(L·d)]
V	reactor volume [L]
υ	stoichiometric mass ratio [g H_2/g NO_3^-—N]
X_f	biofilm density [gVSS/mL]

Since N_2 reaches equilibrium and is not accumulated over time, there is no need for gas discharge and the risky and economic H_2 loss to atmosphere through gas purging of the reactor is prevented. Hydrogen loss is therefore limited only to the dissolved H_2 in the effluent and H_2 utilization efficiencies above 92% were achieved. The operation under low-pressurized headspace consisting uniquely of H_2 and N_2 gases prevents hazardous H_2—O_2 contact and minimizes the risk of explosion in case of failure (Epsztein et al., 2016).

On top of the inherent advantages of safety and economics, the new reactor was designed to ensure high denitrification rates in comparison to existing hydrogenotrophic systems by using high-surface-area plastic carriers and maintaining high mass transfer of H_2 gas. The high mass transfer of H_2 gas can be accomplished by operating the reactor either under an unsaturated flow regime where water is recirculated through the H_2 gas-enriched headspace and trickled over the biofilm carriers (Epsztein et al., 2016), or with submerged bed where gas is recirculated from the headspace to the bottom and bubbled through the submerged bed.

The main objective of the current research is to compare between two types of biofilm reactors using the above hydrogenotrophic denitrification reactor as a case study: a submerged bed reactor (SuBR) and an unsaturated flow reactor (uSFR). The inherent features of the two reactors are discussed with a focus on the effective biofilm surface area and gas-liquid mass transfer.

2. Materials and methods

2.1. Experimental setup

The SuBR was based on the same reactor tank used for the uSFR (Epsztein et al., 2016) as shown in Fig. 1.

The comparison between the two reactors was based on the same packing volume of plastic carriers (total surface of 900 m^2/m^3, Aqwise). However, in order to allow for good mixing and fluidization of the carriers in the SuBR (as in fluidized or moving bed reactor), the carriers filling ratio chosen for the SuBR was ~60% (instead of 100% in the uSFR), and therefore a higher volume of the PVC cylindrical column (diameter of 10.5 cm) was utilized for the SuBR tests (height of 90 cm in the SuBR instead of 51 cm in the uSFR). The reactors were continuously fed with nitrate-contaminated groundwater. The level switches controlling water drainage were located in the reactor's bottom and top part for the unsaturated (i.e. uSFR) and saturated flow mode (i.e. SuBR), respectively. When enough liquid collected at the reactors and reached the level switch, a drainage valve was opened and a portion of treated water was released (i.e. pulsed discharge). A detailed description of the equipment in the uSFR was given earlier (Epsztein et al., 2016). The SuBR was connected to a gas supply (H_2 cylinder with pressure regulator), feed pump (Diaphragm pump model 7090-42, Cole-Palmer), gas recirculation pump (Peristaltic pump model 7553-75, Cole-Palmer), water recirculation pump (optional) (FL-2403, ProPumps) and pH controlling unit (standard pH electrode, pH controller – pH190, Alpha; hydrochloric acid tank and acid pump – gamma/L, ProMinent). Gas recirculation from the reactor's headspace was introduced at the bottom of the reactor through an aquarium-type air diffusion stone.

The feed solution for all experiments was tap water mixed with concentrated stock solutions of $NaNO_3$ and KH_2PO_4. The volumetric flow rate was 450 mL/min and effluent NO_3^--N was controlled by adjusting the inlet NO_3^--N concentration. Water temperature was maintained constant at 27.5 ± 1 °C. Bulk pH was kept at 7 ± 0.1 by dosing hydrochloric acid. Influent, effluent and water from the top part of the reactors were collected for further analyses. All rate calculations in this work were based on the packing volume of the carriers (i.e. $V = 4.4$ L).

2.2. Analytical methods

Nitrate was determined using a Metrohm 761 ion chromatograph (IC) equipped with a 150 mm Metrosep A Supp 5 column with column guard and suppressor using a CO_3^{-2}/HCO_3^- eluent. Nitrite-N and alkalinity were measured according to Standard Methods (Method 4500 and Method 2320, respectively). The total suspended solids (TSS) concentration was also carried out according to Standards Methods (APHA et al., 1995). Total Organic Carbon (TOC) concentration was determined by a TOC-VCPH analyzer (Shimadzu, Kyoto, Japan). DOC concentration was determined by performing TOC analysis on samples filtered through 0.22 mm syringe filter.

2.3. Reactors operation

According to the concept developed, normal reactors operation is done under a constant total pressure (i.e. pressure of H_2 and N_2 gases). In the beginning of the process the partial pressure of N_2 increases and the partial pressure of H_2 decreases till gas-liquid equilibrium is achieved. The partial pressures of H_2 and N_2 gases at equilibrium depend on the amount of NO_3^--N removed per litre of treated water (Epsztein et al., 2016).

In this work the operational conditions were changed according to the specifications of each experiment. When excess of H_2 and NO_3^--N was required, the operation to steady state was performed with the highest gas or liquid recirculation (1.5 and 8 L/min,

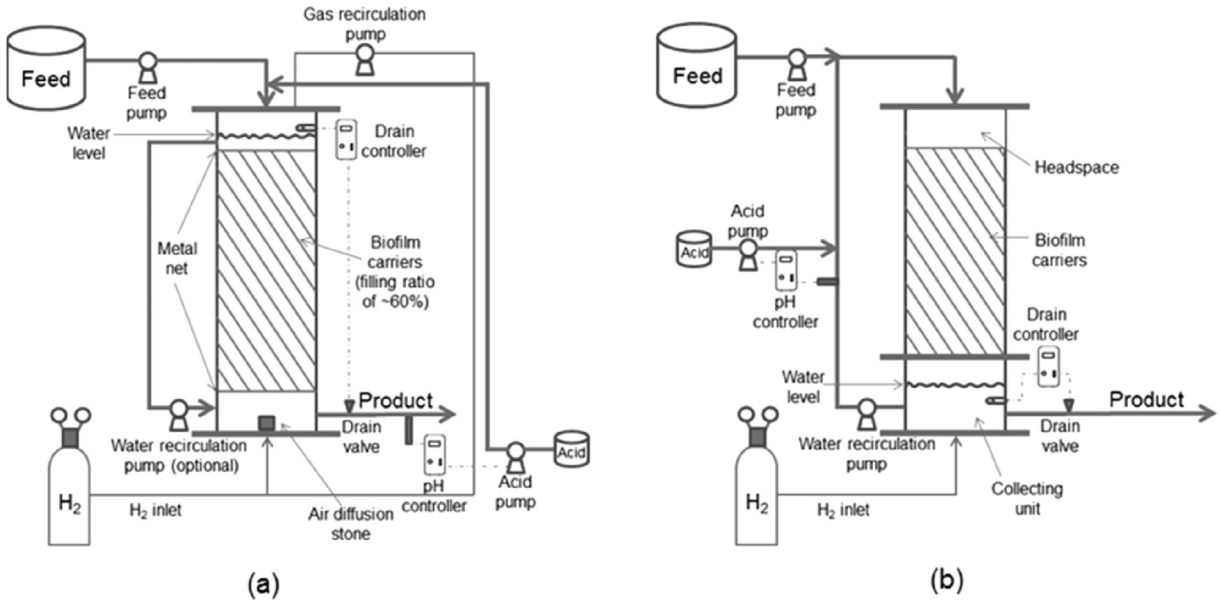

Fig. 1. Schematic diagram of the SuBR (a) and the uSFR (b).

respectively), high effluent NO_3^--N concentration above 20 mg/L and constant H_2 pressure of 2 bars. Only for the experiment purpose, the H_2 pressure was maintained constant by continuous flushing of the reactor's headspace with H_2 gas under pressure of 2 bars to ensure steady-state conditions under a stable and known H_2 pressure within the reactor. For the current research purposes, steady state was defined as an operational state presenting constant denitrification rate during extended operation. At steady state, NO_3^--N concentration was decreased to 10 mg/L to simulate a real treatment process complies with the common worldwide regulations. The specific conditions applied after reaching steady state for comparing the effective biofilm surface area and the overall gas-liquid mass transfer coefficient in the two reactors are described in the next section.

Every few days (see Results and discussion below), the operation was stopped for cleaning. Cleaning included washing of carriers, column and pipes with known and constant amount of tap water.

2.4. Comparison of the effective biofilm surface area A and the overall gas-liquid mass transfer coefficient k_La in the two reactors

For comparing the effective biofilm surface area A in the two reactors, H_2 was given in excess by continuous flushing of the reactor's headspace with H_2 gas under pressure of 2 bars and the effluent NO_3^--N concentration N_e was kept constant at 5 mg/L by adjusting the inlet NO_3^--N concentration N_i in the range of 25–35 mg/L. For assessing k_La, H_2 was set to be limiting (i.e. NO_3^- in excess) by continuous flushing of the reactor's headspace with H_2 gas under a lower pressure of 1.5 bars and keeping the N_e values above 20 mg/L by applying a high N_i above 40 mg/L.

3. Results and discussion

3.1. Main performance characterization of the reactors

The two reactors (SuBR and uSFR) were operated for 60 days each with constant H_2 pressure (2 bars) and gas or liquid recirculation flow rates of 1.5 and 8 L/min, respectively. The influent NO_3^--N concentration was adjusted so that the effluent concentration was 10 mg NO_3^--N/L. The results of the denitrification rates, effluent quality, cleaning frequency and the estimated recirculation energy consumption for the two reactors are summarized in Table 1.

The average denitrification rate in the SuBR was about 75% of the rate achieved in the uSFR with liquid recirculation of 8 L/min (i.e. full media wetting). This value is still one order of magnitude higher than most previous reported rates for hydrogenotrophic denitrification (Epsztein et al., 2016). The reasons for the lower rates in the SuBR may be attributed to the lower effective biofilm surface area and/or the lower gas-liquid mass transfer coefficient, as discussed later. Similar values of effluent DOC were achieved for both reactors. Since the DOC of tap water was 0.7 mg/L, the contribution of the biological treatment to the DOC level in the treated water was always below 1 mg/L in both reactors. Similar DOC results were observed for hydrogenotrophic denitrification performed in a membrane biofilm reactor (MBfR) (Tang et al., 2012). According to hydrogenotrophic denitrification stoichiometry (McCarty, 1972) and the removal of NO_3^--N (31.2 and 41.4 mg/L for the SuBR and the uSFR, respectively), the biomass yield should be 11.5 and 15 mg/L for the SuBR and uSFR, respectively. Effluent suspended solids were 9 ± 4 mg TSS/L for the SuBR, and much less for the uSFR, 1.4 ± 0.2 mg TSS/L, indicating greater solids holdup in the fixed bed media of the uSFR. The effluent TSS was substantially higher in the SuBR reactor due to biofilm sloughing from the shear forces created by the action of gas bubbling and collision of carriers. This allowed for a longer period of reactor operation between cleanings in the SuBR. In contrast, excess biomass built up faster in

Table 1
Main features comparison between the SuBR and the uSFR at steady state with H_2 pressure of 2 bars and gas or liquid recirculation flow rates of 1.5 and 8 L/min, respectively. Influent concentration was adjusted so that the effluent concentration was 10 mg NO_3^-–N/L.

Parameter	SuBR	uSFR
Average denitrification rate [g N/(L·d)]	4.6 ± 0.1	6.1 ± 0.2
Average effluent DOC [mg/L]	1.3 ± 0.2	1.01 ± 0.08
Average effluent TSS [mg/L]	9 ± 4	1.4 ± 0.2
Cleaning frequency [d]	5	2
[a]Recirculation energy consumption [kWh/m^3]	0.11	0.46

[a] Estimation for 100 m^3/h treatment facility.

the uSFR and reactor cleaning to preserve hydraulic conductivity was required every two days rather than five in the SuBR. Finally, based on estimation for 100 m^3/h treatment facility, the energy consumption for liquid recirculation in the uSFR is expected to be more than 4 times higher than the energy consumption for gas recirculation in the SuBR.

A representative cycle (operation between cleanings) showing the change in denitrification rate, effluent DOC and effluent TSS concentration in the SuBR is given in Fig. 2.

The denitrification rate increased from the first day of operation due to biomass growth and acclimation after the cleaning intermission. Afterwards, it stabilized at an average value of 4.6 ± 0.1 g N/(L·d). Except for day 1, the DOC was also stable during operation with values lower than 1.7 mg/L. The relatively higher DOC in the end of day 1 (2.7 mg/L) can be attributed to organics and metabolites that accumulated in the biofilm and were subsequently released after cleaning. The effluent TSS increased gradually during operation with the increase in biofilm growth on the walls and carriers and reached a maximal level of 14.3 mg/L at day 5. At this stage, biofilm growth on the reactor's internal level switch interfered with intermittent effluent release and partial clogging of the screen separating the carriers from the discharge port of the reactor was also observed, requiring reactor cleaning.

3.2. Comparison between the effective biofilm surface area A and the overall gas-liquid mass transfer coefficient k_La in the two reactors

As mentioned above, the lower denitrification rates achieved in the SuBR could theoretically be attributed to the lower effective biofilm surface area and/or the lower gas-liquid mass transfer coefficient. The comparison of these two parameters in the two reactors was performed by analytical solution of simple mass balances, based on the following assumptions: (1) steady-state conditions and planar, one dimensional and completely homogenous biofilm neglecting the boundary layer on the biofilm surface; (2) for the concentration of NO_3^--N and H_2 pressure applied, the degradation of both substrates along the biofilm can be described by an intrinsic zero-order kinetics (Ghafari et al., 2010; Lu and Gu, 2008; Rezania et al., 2005); (3) H_2 transfer limitation by the interfacial gas-liquid layer; (4) close to CSTR conditions.

Following these assumptions, the main equations used for comparing A and k_La in the two reactors were:

Mass balance on NO_3^--N:

$$0 = Q(N_i - N_e) - r_N V \quad (1)$$

Mass balance on dissolved H_2:

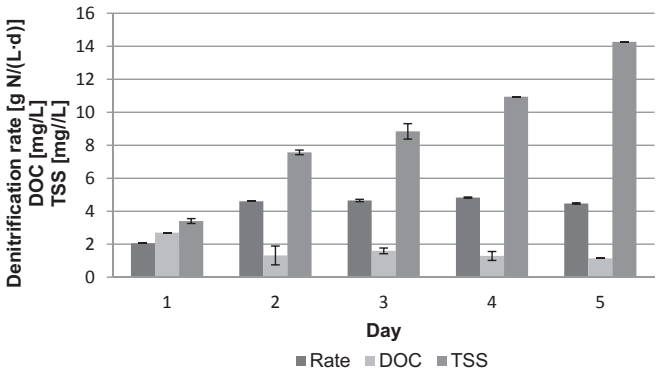

Fig. 2. Denitrification rate, effluent DOC and effluent TSS measured during a representative cycle in the SuBR.

$$0 = k_L\alpha(H^* - H_e)V - QH_e - r_H V \quad (2)$$

The overall NO_3^--N and H_2 degradation rates (r_N and r_H, respectively), based on Harremoes et al. (Harremoes, 1978), in case of:

$$NO_3^- - \text{N limitation} : r_N = A\sqrt{2D_{f,N}k_{0f,N}N_e};\ r_H = \upsilon r_N \quad (3)$$

$$H_2 \text{ limitation} : r_N = \left(\frac{1}{\upsilon}\right) r_H;\ r_H = A\sqrt{2D_{f,H}k_{0f,H}H_e} \quad (4)$$

Where A is the effective biofilm surface area; $D_{f,N}$ and $D_{f,H}$ are the diffusion coefficients of NO_3^- and H_2 in the biofilm, respectively; $k_{0f,N}$ and $k_{0f,H}$ are the degradation rates of NO_3^--N and H_2 in the biofilm, respectively, and equal to $q_{max,N}X_f$ and $q_{max,H}X_f$, respectively; N_e and H_e are the effluent concentrations of NO_3^--N and dissolved H_2 respectively; and υ is the stoichiometric mass ratio (g H_2: g NO_3^--N) which equals to 0.429 g H_2/g NO_3^--N (McCarty, 1972). A full list of parameters is shown in the Nomenclature.

Comparison of A in the two reactors was done by Eq. (3) under conditions of NO_3^--N limitations. Applying the same effluent NO_3^--N concentration (i.e. N_e) in both reactors, and assuming that the product of NO_3^- diffusivity and biofilm density (i.e. $D_{f,N}X_f$) and the maximal specific degradation rate of NO_3^- (i.e. $q_{max,N}$) are identical in both reactors, the difference in r_N between the two reactors depends uniquely on the effective biofilm surface area A. Therefore, the ratio between the values of r_N in the two reactors under conditions of NO_3^- limitation may serve also as a good comparison indicator for A (the value of A itself was not calculated). For the calculation of r_N in the two reactors, H_2 was given in excess and the effluent NO_3^--N concentration N_e was decreased from 10 to 5 mg/L after reaching steady state to ensure NO_3^--N limitation. After stabilization, N_i and N_e were measured and the denitrification rate r_N was calculated by Eq. (1). As discussed above, the ratio between the r_N values in the two reactors gives the ratio between the effective biofilm surface areas A in the two reactors. Equation (3) was used also to calculate the expression of $A\sqrt{2D_{f,N}k_{0f,N}}$ by dividing r_N by $\sqrt{N_e}$. This expression was multiplied by $\sqrt{\upsilon x\left(\frac{D_{f,H}}{D_{f,N}}\right)}$ to get the expression of $A\sqrt{2D_{f,H}k_{0f,H}}$, so it can be used later to calculate k_La (see explanation below).

For assessing k_La values by Eq. (2), H_e values are initially had to be calculated by Eq. (4). In order to use Eq. (4), H_2 was set to be limiting (i.e. NO_3^- in excess) by continuous flushing of the reactor's headspace with H_2 gas under a lower pressure of 1.5 bars and keeping the N_e values above 20 mg/L. The k_La values were assessed for both reactors using the following procedure: (a) N_i and N_e were measured; (b) the denitrification rate r_N was calculated by Eq. (1) and converted to H_2 degradation rate r_H by the stoichiometric mass ratio υ; (c) using Eq. (4), H_e was calculated by dividing r_H by the value of $A\sqrt{2D_{f,H}k_{0f,H}}$ calculated earlier under conditions of NO_3^--N limitation; (d) the overall volumetric gas-liquid mass transfer coefficient k_La was calculated analytically by Eq. (2) using the corresponding H^* for H_2 pressure of 1.5 bar according to Henry's law (i.e. $H^* \approx 2.3$ mg/L).

The results of the comparison of A and k_La in the two reactors showed that: (1) the A value calculated in SuBR was 89% of the value calculated in the uSFR; (2) the k_La value in the SuBR was approximately 60% of the value calculated in the uSFR (764 vs. 1216 1/d, respectively).

The lower values of both A and k_La in the SuBR can explain the

lower denitrification rates achieved in this system compared to the uSFR. The relatively low value of k_La ($k_La = \frac{D}{\delta}a$) in the SuBR can be attributed to an increased gas-liquid boundary layer δ or/and a decreased specific interfacial area a. In the uSFR, it was shown that higher liquid recirculation affects k_La by increasing α and decreasing δ (Epsztein et al., in press). In the SuBR, the type of diffuser, gas recirculation intensity and reactor geometry may strongly affect the mixing efficiency (controls δ), the number and size of emerging bubbles (controls a) and collision and merging of bubbles (controls a). It is possible that the relatively long-narrow column used in this work affected mixing conditions and resulted in merging bubbles and therefore might be more adequate for trickling system (i.e. uSFR) than for bubbling one (i.e. SuBR).

Further investigation was performed in order to assess whether the lower k_La values calculated in the SuBR originated from limitation by the gas-liquid boundary layer δ and/or the specific interfacial area a. This investigation was carried out by exploring the effect of the gas recirculation flow rate on k_La as discussed in the next section.

3.3. Effect of gas recirculation flow rate on the overall gas-liquid mass transfer coefficient k_La in the SuBR

As discussed in the former section, the gas recirculation intensity may affect both the mixing conditions (with the accompanied effect on δ) and the nature of the emerging bubbles (with the accompanied effect on a). Therefore, in order to better understand whether the lower k_La values calculated in the SuBR originated from limitation by δ and/or α, the effect of gas recirculation flow rate on k_La was investigated under conditions of H_2 limitation.

In this specific experiment a high liquid recirculation was added to the SuBR to ensure CSTR conditions and allow the use of Eqs. (1) and (2) independently of the gas recirculation flow rate. After operating the reactor to steady-state (see Reactors operation above) with the addition of liquid recirculation, the gas recirculation flow rate was decreased gradually and for each gas recirculation flow rate the k_La was calculated using the same procedure described in the former section.

Under the high mixing conditions provided by adding the high liquid recirculation, the k_La observed at the normal gas recirculation flow rate (1.4–1.5 L/min) was significantly improved (from 764 to 1043 1/d). This improvement indicates mixing limitation with the accompanied higher δ under normal operational conditions (before the addition of liquid recirculation). The effect of gas recirculation flow rate on k_La and denitrification rate is shown in Fig. 3.

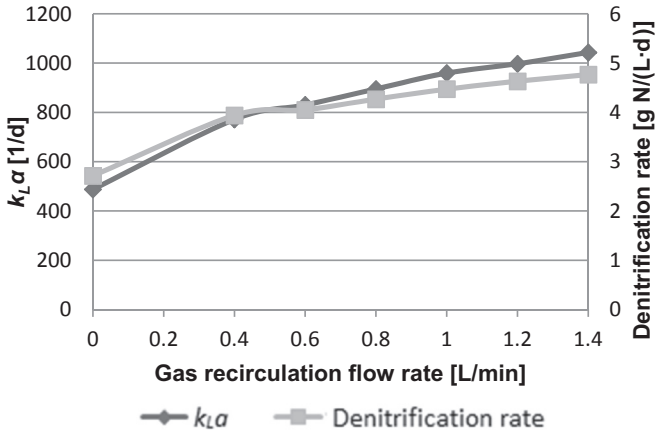

Fig. 3. k_La values and denitrification rates calculated for different gas recirculation flow rates in the SuBR.

Under high hydraulic mixing conditions, Fig. 3 shows that k_La values deteriorated with lower gas recirculation flow rates. The decrease in k_La values was accompanied by gradual decrease in denitrification rates, thus strengthening the claim that the reactor was operated under H_2 limitation conditions. Knowing that hydraulic mixing was high enough throughout this experiment (due to the high liquid recirculation), the decrease in k_La values with lower gas recirculation flow rates can be explained by the decrease in a (and not in δ). Apparently, with higher gas recirculation flow rates, more bubbles emerge from the diffuser, thus enlarging the interfacial area a and also the k_La value. Pittoors et al. also demonstrated improved k_La values for higher airflow rates and explained it by the increased bubble density with the accompanied increased interfacial area α and driving force with higher airflow rates. In addition, with higher airflow rates turbulence and agitation increase and bubble breakage is promoted (Pittoors et al., 2014). The results in this section show that the k_La observed in the SuBR at normal operational conditions was limited by both δ and α.

4. Conclusions

Comparison between gas recirculation-based reactor (SuBR) and liquid recirculation-based reactor (uSFR) in a pressurized closed-headspace hydrogenotrophic denitrification system showed lower denitrification rates in the SuBR than in the uSFR (4.6 vs. 6.1 g N/(L·d)). Yet, these rates are one order of magnitude higher than most previous reported rates for hydrogenotrophic denitrification. The SuBR presented also lower effluent quality based on suspended solids due to biofilm sloughing from the shear forces created by the action of gas bubbling and collision of carriers in the SuBR. On the other hand, this phenomenon of biofilm sloughing allowed for more stable and longer operation in the SuBR with reactor cleaning every five days, as compared to reactor cleaning every two days in the uSFR. Moreover, the recirculation energy consumption in the SuBR is estimated to be ~25% of that in the uSFR. The lower denitrification rates in the SuBR were found to result from lower effective biofilm surface area and overall gas-liquid mass transfer coefficient k_La in the SuBR. The k_La achieved in the SuBR was found to be limited by both the gas-liquid boundary layer δ and the interfacial area a. This can be attributed to the specific system used (i.e. column geometry, type of diffuser, intensity of gas recirculation) affecting both parameters (δ and a). It is possible that the unsaturated flow in the uSFR allows for higher specific interfacial area a due to the high surface area of the carriers (compared to that of the bubbles) and higher k_La due to the high diffusivity of H_2 in the gas phase of the uSFR. In conclusion, the comparison showed that each reactor has its own advantages and drawbacks based on the specific conditions of the systems tested. Yet, at this stage of development it seems that the submerged system advantages make it the preferred choice for full scale implementation.

References

APHA, AWWA, WPCF, 1995. Standard Methods for the Examination of Water and Wastewater, nineteenth ed. Washington DC.

Daigger, G.T., Boltz, J.P., 2011. Trickling filter and trickling filter– suspended growth process design and operation: a state-of-the-art review. Water Environ. Res. 83, 388–404. http://dx.doi.org/10.2175/106143010X12681059117210.

Eding, E.H., Kamstra, A., Verreth, J.A.J., Huisman, E.A., Klapwijk, A., 2006. Design and operation of nitrifying trickling filters in recirculating aquaculture: a review. Aquac. Eng. http://dx.doi.org/10.1016/j.aquaeng.2005.09.007.

Epsztein, R., Beliavski, M., Tarre, S., Green, M., 2016. High-rate hydrogenotrophic denitrification in a pressurized reactor. Chem. Eng. J. 286, 578–584.

Epsztein, R., Beliavski, M., Tarre, S., Green, M., Simplified model for

hydrogenotrophic denitrification in an unsaturated-flow pressurized reactor. Chem. Eng. J. in press.
Ghafari, S., Hasan, M., Aroua, M.K., 2010. A kinetic study of autohydrogenotrophic denitrification at the optimum pH and sodium bicarbonate dose. Bioresour. Technol. 101, 2236–2242. http://dx.doi.org/10.1016/j.biortech.2009.11.068.
Harremoes, P., 1978. Biofilm kinetics. Water Pollut. Microbiol. 2, 71–109.
Lekang, O.I., Kleppe, H., 2000. Efficiency of nitrification in trickling filters using different filter media. Aquac. Eng. http://dx.doi.org/10.1016/S0144-8609(99)00032-1.
Lu, C.X., Gu, P., 2008. Hydrogenotrophic denitrification for the removal of nitrate in drinking water. Huanjing Kexue/Environ. Sci. 29, 671–676.
McCarty, P.L., 1972. Stoichiometry of biological reactions. In: Proceedings of the International Conference towards a Unified Concept of Biological Waste Treatment Design. Atlanta, Georgia.
Pittoors, E., Guo, Y., Hullen, S.W.H. Van, 2014. Modeling dissolved oxygen concentration for optimizing aeration systems and reducing oxygen consumption in activated sludge processes: a review. Chem. Eng. Comm. 201, 983–1002.
Rezania, B., Cicek, N., Oleszkiewicz, J.A., 2005. Kinetics of hydrogen-dependent denitrification under varying pH and temperature conditions. Biotechnol. Bioeng. 92, 900–906. http://dx.doi.org/10.1002/bit.20664.
Schlegel, S., Koeser, H., 2007. Wastewater treatment with submerged fixed bed biofilm reactor systems - design rules, operating experiences and ongoing developments. Water Sci. Technol. http://dx.doi.org/10.2166/wst.2007.245.
Tang, Y., Ziv-El, M., Meyer, K., Zhou, C., Shin, J.H., Ahn, C.H., McQuarrie, J., Candelaria, D., Swaim, P., Scott, R., Rittmann, B.E., 2012. Comparing heterotrophic and hydrogen-based autotrophic denitrification reactors for effluent water quality and post-treatment. Water Sci. Technol. Water Supply 12, 227–233. http://dx.doi.org/10.2166/ws.2012.138.